Fracture Toughness of Sharply Notched Specimens in the Ductile-to-Brittle Transition Regime of Ferritic Steel

Hans-Jakob Schindler[1,a], Dietmar Kalkhof[2,b] and Hans-Werner Viehrig[3,c]

[1] Mat-Tec AG, Unterer Graben 27, CH-8401 Winterthur, Switzerland

[2] Swiss Federal Nuclear Safety Inspectorate, CH-5200 Brugg, Switzerland

[3] Helmholtz-Zentrum Dresden-Rossendorf, Dresden, Germany

[a] schindler@mat.tec.ch, [b] dietmar.kalkhof@ensi.ch, [c] h.w.viehrig@hzdr.de

Keywords: Ductile to brittle transition, reference temperature, notch, toughness, root radius, ferritic steel

Abstract. The fracture behavior of a component or specimen that contains a sharp notch is governed essentially by the same theoretical relations known from fracture mechanics of solids with cracks. The notch root radius only causes an increase of the resistance against crack initiation. In the present paper, the relation between fracture toughness and notch toughness is investigated experimentally. The effect of the notch radius on fracture toughness depends on the fracture mechanism. It is most pronounced in the brittle to ductile transition regime, where fracture toughness can be characterized by the Master-Curve (MC) and the corresponding reference temperature T_0 according to ASTM E1921. Accordingly, the effect of the notch radius can be quantified by a shift of T_0. The corresponding relations are considered analytically by means of simple models as well as experimentally by CT- and SEB-specimens that contained a sharp notch with ρ=0.06 mm introduced by spark erosion (EDM) instead of the standard fatigue crack. Dynamic and quasi-static loading was considered. In all cases the difference ΔT_{0N} between the standard T_0 and the corresponding reference temperatures of the notched specimens, T_{0N}, turned out to be approximately the same.

Introduction

Engineering fracture mechanics usually deals with the fracture behavior of structural components in the presence of a crack. However, sometimes there are sharp notches present rather than cracks, for example in cases of corrosive or mechanical surface damage. Concerning fracture toughness testing, there are situations where introducing a well-defined fatigue crack is difficult and expensive, for example if the crack tip shall be placed in a certain narrow region, like the heat affected zone of a weldment. Sharp notches machined by Electric discharge machining (EDM) are also suitable to represent a well defined surface flaw in component testing. In such cases sharp notches can serve as simpler and less expensive substitutes of a crack. However, the initiation toughness is affected by the notch root radius. To predict the fracture load of a notched component or to estimate fracture toughness from testing a notched specimen, the effect of the root radius ρ (see Fig. 1) on fracture toughness has to be known.

The effect of ρ on fracture toughness is likely to be not unique, but dependent on the fracture mechanism. In general, the most sensitive toughness range regarding influencing factors is the brittle-to-ductile transition (DBT). In the present paper, emphasis is placed on this toughness range, including the adjacent regions of upper and lower shelf. In the DBT-range fracture toughness is affected by a pronounced natural scatter, so probabilistic methods have to be applied for the evaluation of test data. In case of ferritic steels, fracture toughness in the DBT-regime can be characterized by the reference temperature T_0 based on the MC approach [1, 2]. Compared with a crack, a notch with a specific root radius is expected to cause a shift of T_0 to lower temperatures.

The present investigation includes both experimental and theoretical investigations. The experiments are documented in detail in [3] and in condensed form in [4]. In the present paper the experimental results are further analyzed and compared with theoretical relations derived by means of simple analytical models. The corresponding theoretical relations enable the experimental results to be generalized and fracture toughness to be estimated from test on sharply notched specimens.

Theoretical Considerations

General. In presence of a sharp notch, which means that its root radius ρ is at least one order of magnitude smaller than its depth a (see Fig. 1), the fracture behavior of a component is in principal similar to that of a crack, which can be defined as a notch with ρ=0. Thus, the same theoretical concepts of linear-elastic (LEFM) or elastic-plastic (EPFM) fracture mechanics, respectively, can be applied to predict the fracture load. However, the resistance against crack initiation (called subsequently notch toughness and denoted by K_{Nc}) depends on the notch radius. To investigate the effect theoretically, one has to distinguish at least between upper shelf, lower shelf and DBT-behaviour. In all cases, basic models as simple as possible are used.

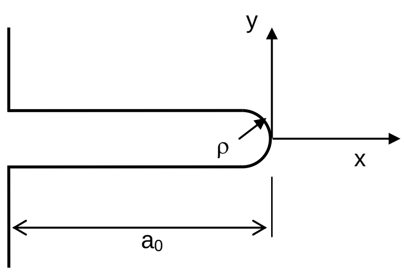

Fig. 1: Geometry of a sharp edge notch of depth a0 and root radius r

Lower Shelf. In the lower shelf region, initiation of crack extension is governed by the local stress. Its maximum value σ_N is given by

$$\sigma_N = \sigma_y(x=0) = \frac{2K_I(a_0)}{\sqrt{\pi \cdot \rho}} \quad (1)$$

Crack initiation requires $\sigma_N = \sigma_c*$, where σ_c* denotes the cleavage stress, and unstable crack propagation $K_I = K_{Ic}$. These two criteria lead to the following dependence of notch toughness on ρ:

$$K_{Nc} = \frac{\sigma_c^*}{2} \cdot \sqrt{\pi \cdot \rho} \qquad \text{for} \quad \rho > \rho_c = \frac{4}{\pi} \cdot \left(\frac{K_{Ic}}{\sigma_c^*} \right)^2 \quad (2a)$$

$$K_{Nc} = K_{Ic} \qquad \text{for} \quad \rho \le \frac{4}{\pi} \cdot \left(\frac{K_{Ic}}{\sigma_c^*} \right)^2 \quad (2b)$$

According to (2), K_{Nc} is matching with standard K_{Ic} for very sharp notches ($\rho < \rho_c$). This behaviour is qualitatively confirmed by test on ceramics [6].

Upper Shelf. Fig. 2 shows schematically the vicinity of a notch right at the incident of crack initiation. The shaded triangular area next to the root radius represents the fracture process zone, which is characterized by a strain-softening of the corresponding material. J-Integral is calculated along the dotted path Γ, consisting of the sections $\Gamma_1 - \Gamma_6$. Γ_1 and Γ_6 do not contribute to J. At crack initiation, the material at the root surface is expected to be strained nearly up to its plastic capacity, which means the strain energy per unit volume reaches the specific fracture energy U_f, which is defined to be the area under the true stress-strain curve. This assumption leads to

$$J(\Gamma_2,\Gamma_5) \cong c_1 \cdot U_f \cdot \rho . \tag{3}$$

where c_1 is a non dimensional factor of about 1. U_f can be estimated from a uniaxial tensile test to be

$$U_f \approx \frac{R_m}{1-A_5/100} \cdot \ln\left(\frac{1}{1-Z/100}\right) \tag{4}$$

with R_m being the ultimate tensile strength, A_5 the standard fracture strain and Z the reduction in area at fracture (in %). Integration along the sections Γ_3 and Γ_4 delivers – like in the case of a crack with ρ=0 - $J(\Gamma_3,\Gamma_4) = m \cdot \sigma_f \cdot \delta$ [7], so J required for crack initiation is obtained to be

$$J_{iIN} = J_i(\rho = 0) + \Delta J_{RN} = m \cdot \sigma_f \cdot \delta + c_1 \cdot U_f \cdot \rho \tag{5}$$

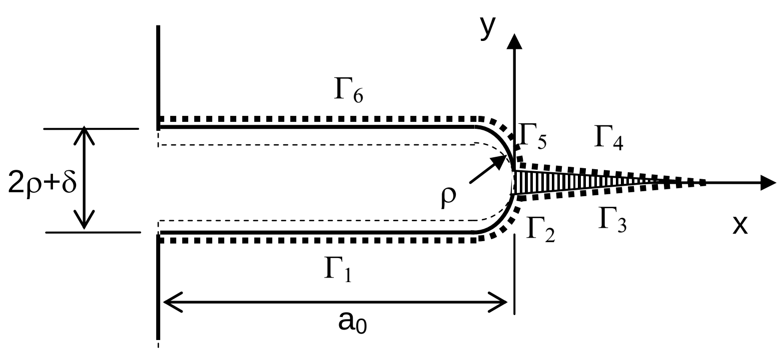

Fig. 2: Notch at the instant of crack initiation, with integration path Γ (consisting of sections Γ_1 – Γ_6) to calculate J.

Ductile-to-brittle transition. Fig. 3a shows qualitatively the well-known stress distribution in front of a crack. With the horizontal axis normalized by J/σ_f (with σ_f being the effective yield stress, defined as the mean value of ultimate tensile strength R_m and yield stress $R_{p0.2}$) and the vertical axis by σ_f, the curve is nearly independent of the loading state quantified by J. Correspondingly, the stress peak $\gamma \cdot \sigma_f$ is nearly independent of J, tending to decrease with increasing J because of plasticity-induced loss of constraints. In the case of a perfect crack, the stress peak occurs at a distance $x^* = c_2 \cdot \delta$, with $c_2 \approx 1.5$ [8]. Cleavage requires two conditions to be fulfilled [9]: (i) the stress peak has to reach the effective cleavage stress, i.e. $\gamma \cdot \sigma_f > \sigma^*_c$, and (ii), x* has to exceed a certain minimum value. In the case of a sharp notch, the stress peak occurs at a larger distance from the notch root, since the full constraints can only develop at a certain minimum distance from the notch root. For dimensional reasons it is likely to assume that the stress peak is shifted to $x^*_N = c_2 \cdot \delta + c_3 \cdot \rho$, with c_3 being a non dimensional constant of the order of 1. In order to shift the stress peak from x* to x^*_N an increase of J is required. For dimensional reasons and by analogy with the case of a crack (ρ=0) the increased J can be assumed to be

$$J_{cN} = J_c + c_3 \cdot \rho \cdot m \cdot \sigma_f = J_c + \Delta J_{cN} \tag{6}$$

where m is the constraint factor that appears in the relation $J = m \cdot \sigma_f \cdot \delta$ in the case of a crack (see eq. (5)), which takes a value of about m≈2 for plane strain or m ≈1 for plane stress conditions, respectively. In the DBT-range, fracture toughness is usually expressed in terms of K_I, which is obtained from (6) by the basic relation

$$K_{cN} = \sqrt{\frac{J_{cN} \cdot E}{1-\nu^2}} = \sqrt{K_{Jc}^2 + \frac{c_3 \cdot \rho \cdot m \cdot \sigma_f \cdot E}{1-\nu^2}} \tag{7}$$

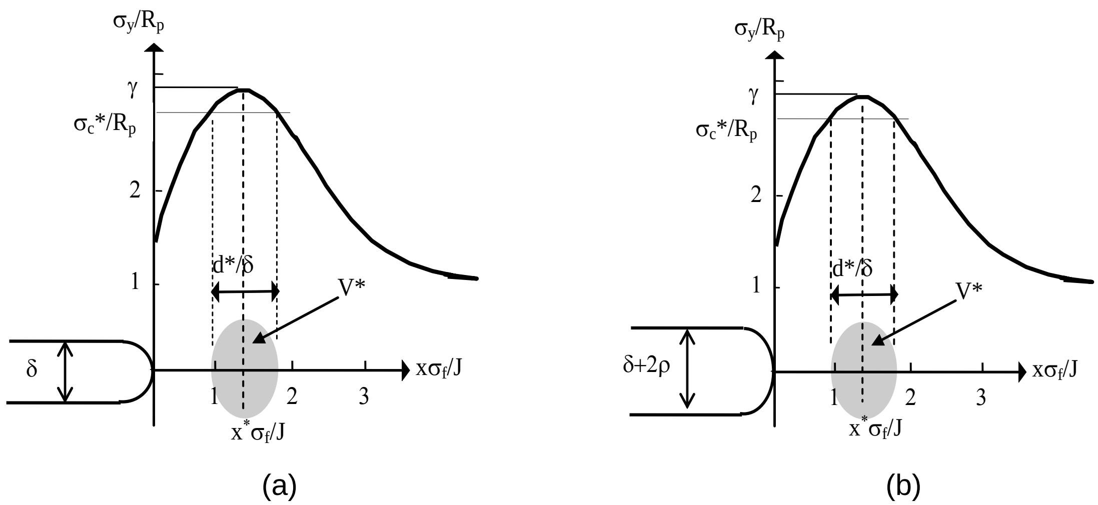

Fig. 3: Stress distribution in front of a crack (a) and a sharp notch (b)

Eq. (7) predicts the curve $K_{JcN}(T)$ to be flatter than $K_{Jc}(T)$, since the effect of the second term under the square root decreases with increasing K_{Jc}. As they approach the transition to upper shelf, K_{JcN} and K_{Jc} tend to coincide. The transition temperature to upper shelf behaviour, which occurs if the condition (i) is no longer fulfilled, is not significantly shifted by ρ. At the left hand side of the DBT-regime, i.e. at the transition to lower shelf, the K_{Jc} and K_{JcN} also tend to coincide due to eq. (2b). Thus, the shape of the transition curve is expected to be not of the common exponential shape as the transition curves of cracked specimen (see eq. (8)), but distorted to an S-shape.

Determination of Reference Temperature T_0. In the DBT-regime the fracture toughness can be characterized by the reference temperature T_0 [1]. The underlying MC- approach is based on the empirical finding that the median K_{Jc} of ferritic steel follows a unique curve of the form:

$$K_{Jc}(T) = 30 + 70 \cdot \exp\left[0.019 \cdot (T - T_0)\right] \tag{8}$$

Since the median $K_{Jc}(T)$ follows (8) it is evident from eq. (7) and the discussion above that the median $K_{JcN}(T)$ does not follow (8). So the condition to apply the procedure prescribed in [1] are not fulfilled in the case of notched specimens. Anyway, an analogous reference temperature T_{0N} can be defined as the temperature where the median K_{JcN} takes the value K_{JcN} = 100 $\mathrm{MPam}^{0.5}$. If test data are relatively close to T_0, then the procedure of [1] can still be applied as an approximation. In general, however, it is recommended to determine T_{0N} by the procedure described in [10, 11], where the coefficient in eq. (8) is not fixed at 0.019, but considered as an open parameter to be determined by a fitting procedure.

The shift of the reference temperature due to the notch radius, $\Delta T_{0N}=T_0-T_{0N}$, can be estimated theoretically as follows. According to (7) and (8) the median K_{JN} at $T=T_0$ is

$$K_{JcN}(T_0)=\sqrt{100^2+\frac{c_3\cdot\rho\cdot m\cdot\sigma_f\cdot E}{1-\nu^2}} \tag{9}$$

Denoting the mean slope of $K_{JcN}(T)$ between $T=T_{0N}$ and $T=T_0$ by s_0, T_{0N} can be estimated by

$$\Delta T_{0N}=T_0-T_{0N}\cong\frac{K_{JcN}(T_0)-100}{s_0} \tag{10}$$

The mean slope s_0 can be assumed to be about equal to the derivative of (8) at $T=T_0$, thus

$$s_0=\frac{dK_{Jc}}{dT}(T_0)=70\cdot 0.019=1.33\frac{MPa\cdot m^{0.5}}{°C} \tag{11}$$

Experimental Data

Test material and specimens. As test material, the pressure vessel steel 22NiMoCr 3-7 was chosen. The main properties are given in Table 1. Standard CT-specimens with B=25.4mm (1T CT) and single edged bend specimens (SEB) with square cross-sections (W=B), i.e. pre-cracked Charpy size specimens, were machined from a forged ring segments of about 250 mm thickness.

Table 1: Tensile properties of test material at room temperature

Temperature [°C]	Yield stress $R_{p0.2}$ [0.2 MPa]	UTS R_m [MPa]	Fracture strain A5 [%]	Red. in area Z [%]
RT	429	583	25	68
-75°C	492	670	28.5	67

An EDM cut was introduced instead of a standard fatigue crack. The diameter of the wire was 0.1 mm, which lead to a slit width of 0.12 mm, thus a root radius of ρ=0.06 mm. For comparison, the same specimens were also provided with a standard fatigue crack. The Charpy-sized SEB-specimens were loaded quasi-statically and dynamically. Dynamic loading was applied by means of an instrumented impact pendulum hammer

Upper shelf. Fig. 4 shows the J-R-curves measured on two EDM-notched 1T-CT-specimens in comparison with the ones of standard fatigued cracked specimens. Whereas the two curves of the notched specimens nearly coincide, the one of the cracked specimens deviate significantly from each other, indicating a better reproducibility of notched specimens. The corresponding blunting lines are estimated as the regression lines in the initially straight part of the curves. As expected, the blunting lines of the EDM-notched specimens are significantly steeper than those with pre-cracks,. By the deviation from the blunting line (BL and BL_N) one can estimate the initiation of crack extension. For comparison the mean curves of each two J-R-curves from Fig. 4 are shown in Fig. 5. The difference ΔJ_R between them starts to increase at about crack initiation of the pre-cracked specimens and flattens out after crack initiation at the notched specimens, as predicted theoretically. Correspondingly, ΔJ_{RN} defined in eq. (5) can be identified in Fig. 5 as the difference of J at the intersection with the 0.2mm off-set blunting line (J_{Ic}) according to ASTM E1820 with the J-R-curve of the notched specimens.

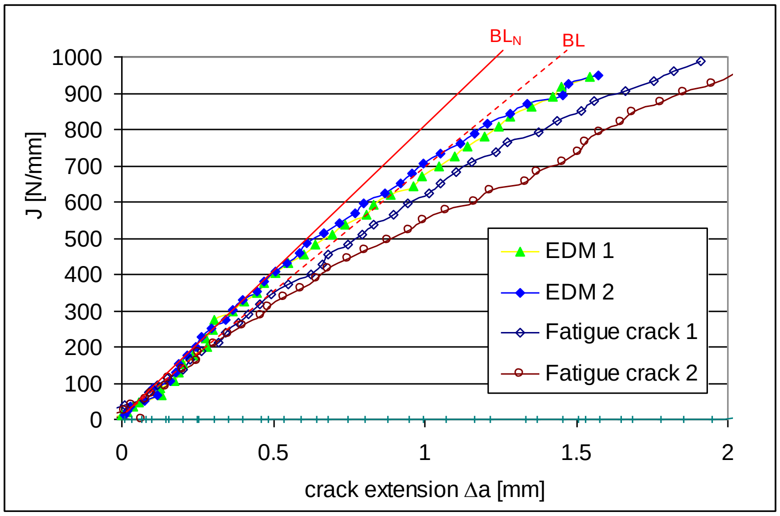

Fig. 4: J-R-curves of two notched 1T-CT-specimens in comparison with J-R-curves of two standard fatigue-cracked 1T-CT-specimens

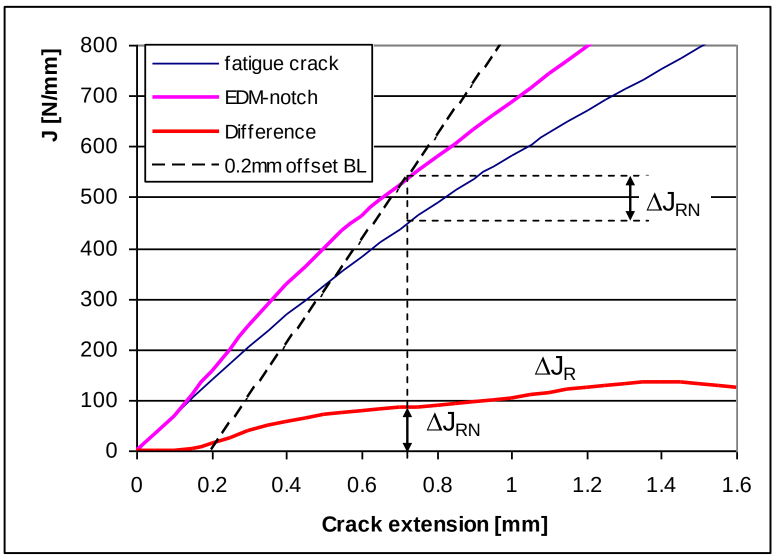

Fig. 5: Mean J-R-curves (from the 2 tests shown in Fig. 4) and the difference of J as a function of crack extension

Fracture toughness in the DBT-range. Fig. 6 shows the K_{Jc} values obtained from a series of EDM-notched 1T-CT- and 0.4T-SEB specimens with two different crack lengths, a=0.5W and 0.3W. They are compared with the data of the same specimens with standard fatigue cracks. Fig. 6 shows the comparison for the 0.4T-SEB specimens under impact loading (impact velocity 1.2 m/s) by using a standard Charpy pendulum hammer, which corresponds to a loading velocity of about $dK_J/dt = 10^5$ $MPa{\cdot}m^{0.5}/s$. The reference temperatures T_{0N} of each specimen type and loading condition were evaluated according to ASTM E1921 [1], disregarding the concerns discussed above about the applicability of this procedure to the notched specimens. The results are shown in Table 2. The shift in T_0 , ΔT_{0N}, due to the notch is about 40K – 50K in all cases. Regarding the standard deviation of the T_0-values of about 8°C [1], the shift can be considered as essentially constant. Its mean value is ΔT_{0N} = -47K.

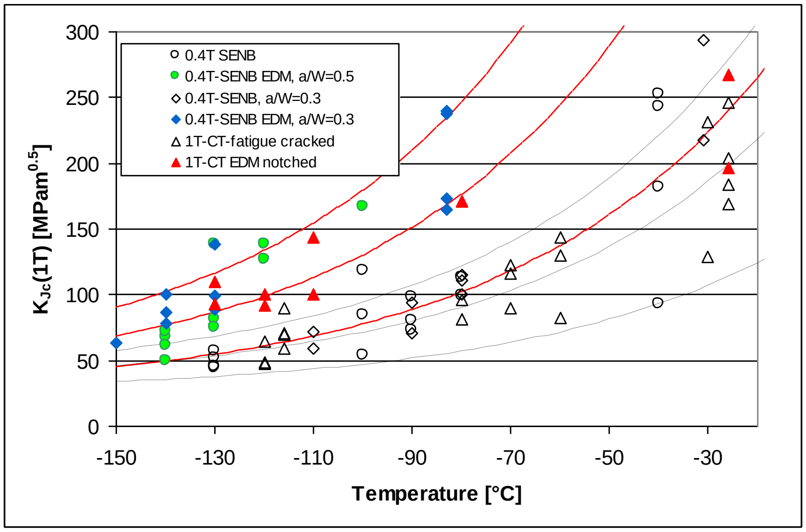

Fig. 6: Experimental K_{Jc}-and K_{JcN}- values size adjusted to 1T as a function of test temperature, with median, 5%- and 95% tolerance bounds according to [1].

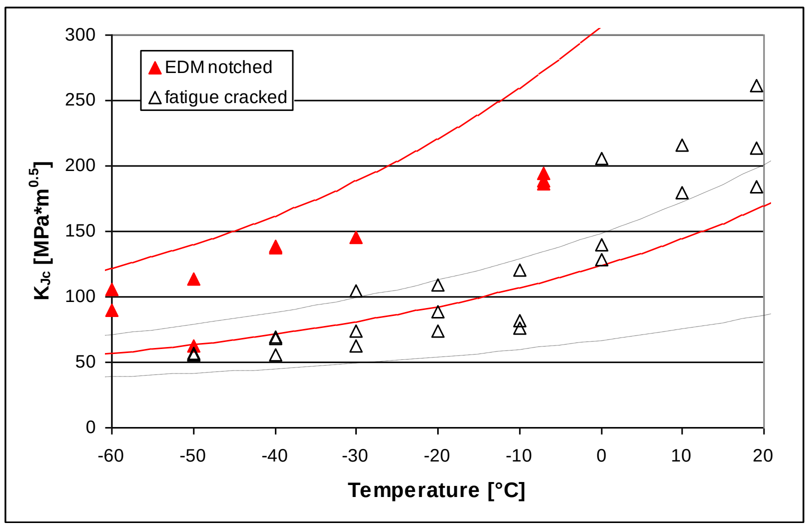

Fig. 7: Impact test results of 0.4T-SEB-specimens, with 5% and 95% tolerance bounds.

Table 2: Reference temperatures T_{0N} in comparison wit T_0, and the corresponding shift ΔT_{0N}.

	T_{0N} EDM	T_0 fatigued	ΔT_{0N}
1T CT	-119	-72	-47
0.4T SEB-a/W=0.5	-127	-86	-41
0.4T SEB-a/W=0.3	-131	-78	-54
0.4T SEB-0.5 impact	-55	-6	-49

Discussion and Conclusions

In Fig. 6 and 7 one can recognize the predicted tendency to an S-shaped distortion of the transition curve. Note that the data of the fatigued specimens under impact loading leave the tolerance band for $T>T_0$ (see [10, 11]), whereas the data of the notched specimens stay within the band. Thus, determination of T_{0N} according to [1] can lead to errors, if the test temperature is not close to T_{0N}.

To overcome this problem it is recommended to use the OEF-method explained in [10, 11], where the actual shape of the median determined by the experimental data is used instead of eq. (8).

The experimental data can be explained by simple theoretical models. . A shift of the reference temperature due to the notch of ΔT_{0N} = 47 K is obtained from eqs. (9) – (11) by inserting the material properties from Table 1 and choosing m=2 and c_3=1.2, which are physically reasonable values of these parameters. Based on these results it is possible to estimate T_0 from tests on EDM-notched specimens. T_0 can be found either by T_{0N} and the shift ΔT_{0N} according to eq. (10), or by correcting the experimental J_{cN} values to J_c by means of eq. (6) and applying the standard MC-procedure to the corresponding K_{Jc}-values. Concerning ΔJ_{cN}, which is required to correct J_{cN} according to eq. (6): Inserting the material parameters from Table 1 in eq. (4) reveals that U_f and σ_f are of the same order of magnitude. Since c_1 and c_3 have also similar values, ΔJ_{RN} according to eq. (5) and ΔJ_{cN} according to eq. (6) are numerically similar, too,, which is confirmed by the presented experimental data. This opens the possibility to determine ΔJ_{cN} approximately by two R-curves as shown in Fig. 5, using $\Delta J_{cN} \approx \Delta J_{RN}$.

It is interesting to note that the deviation of T_0 between 1T-CT-specimens and 0.4T-SEB-specimens, which is mentioned in [3] as a bias, is about the same for EDM-notched specimens. This confirms the systematic nature of this effect, which is explained in [10, 11].

References

[1] American Soc. For Testing and Materials, Standard Test Method for Determination of Reference Temperature, *To*, for Ferritic Steels in the Transition Range, ASTM Standard E 1921-11, West Conshohocken, PA, 2011

[2] Wallin, K, “Recommendation for Application of Fracture Toughness Data for Structural Integrity Analysis,” Proc. CSNI/IAEA Specialists' Meeting, Oak Ridge, TN, 1992

[3] Zurbuchen, C., Viehrig, H.W., Bruchmechanische Werkstoffcharakterisierung zur Überwachung der Neutronenversprödung von Reaktordruckbehältern, Forschungszentrum Dresden, Institutsbericht FZD/FWS/2009/07, Revision 1, August 2010

[4] Viehrig H.W., Schindler H.J., Kalkhof, D., Effects of Test Parameters on the Master Curve Reference Temperature, 18^{th} Europ. Conf. on Fracture (ECF 18), Dresden, 2010

[5] Schindler, H.J., Dauerfestigkeitsnachweis für gekerbte Bauteile mit Imperfektionen unter Anwendung bruchmechanischer Beziehungen und Schwellenwerte, DVM-Bericht 234, pp. 67-76, 2002

[6] R.J. Primas e R. Gstrein, "ESIS TC-6 ROUND-ROBIN ON FRACTURE-TOUGHNESS", Fatigue & fracture of engineering materials & structures, 20(4), 1997, pp. 513-532

[7] Rice, J.R., A mathematical theory of fracture, in: Fracture: an Advanced Treatise, Ed. H. Liebowitz, Academic Press, 1969

[8] Anderson, T.L. Fracture Mechanics: Fundamentals and Applications, CRP Press, 4^{th} Edition, 2003

[9] Ritchie, R.O, Knott, F.F., Rice, J, , J. Mech. Phys. Solids, 21, 395-410, 1973

[10] Schindler, H.J, Kalkhof, D., Size and Rate Effects on Reference Temperature T_0, to be published

[11] Kalkhof, D., Schindler, H.J., Uncertainties in T_0 and Required Safety Margins in Lower Bounds of KIc in the Ductile-to-Brittle Transition Regime of Ferritic Steels, Proc. 19^{th} European Conference on Fracture (ECF19), Paper ID 257, Kazan, RU, 2012